Biochimica et Biophysica Acta 1798 (2010) 1767–1778

Contents lists available at ScienceDirect

Biochimica et Biophysica Acta

journal homepage: www.elsevier.com/locate/bbamem

Erythrocyte morphological states, phases, transitions and trajectories

Sergey V. Rudenko *

Institute for Problems of Cryobiology and Cryomedicine, National Academy of Sciences of the Ukraine, 61015 Kharkov, Pereyaslavskaya Str. 23, Ukraine

ARTICLE INFO

Article history:
Received 10 February 2010
Received in revised form 19 April 2010
Accepted 7 May 2010
Available online 8 June 2010

Keywords:
Red blood cell
Morphological response
Shape
Low ionic strength
Anion
pH

ABSTRACT

Morphological response (MR) of red blood cells represents a triphasic sequence of spontaneously occurring shape transformation between different shape states upon transfer the cells into isotonic sucrose solution in the order: S_0 (initial discoid shape in physiological saline) → S_1 (echinocytic shape at the beginning of MR, phase 1) → S_2 (intermediate discoid shape, phase 2) → S_3 (final stomatocytic shape, phase 3). In this paper, the dynamics of cell shape changes was investigated by non-invasive light fluctuation method and optical microscopy. Among 12 possible transitions between four main shape states, we experimentally demonstrate here an existence of nine transitions between neighbour or remote states in this sequence. Based on these findings and data from the literature, we may conclude that red blood cells are able to change their shape through direct transitions between four main states except transition $S_1 \rightarrow S_0$, which has not been identified yet. Some shape transitions and their temporal sequence are in accord with predictions of bilayer couple concept, whereas others for example transitions between remote states $S_3 \rightarrow S_1$, $S_1 \rightarrow S_3$ and $S_3 \rightarrow S_0$ are difficult to explain based solely on the difference in relative surface areas of both leaflets of membrane suggesting more complex mechanisms involved. Our data show that MR could represents a phenomenon in which the major role can play pH and chloride-sensitive sensor and switching mechanisms coupled with transmembrane signaling thus involving both cytoskeleton and membrane in coordinated shape response on changes in cell ionic environment.

© 2010 Elsevier B.V. All rights reserved.

1. Introduction

Under physiological conditions, a normal human RBC assumes a biconcave discoid shape. It is well known that a variety of agents can modify this shape systematically and reversibly at constant area and volume ([1–4] and references therein). One set of agents, including anionic amphipaths, high salt, high pH, ATP depletion, cholesterol enrichment and proximity to a glass surface, induces a series of crenated shapes, called echinocytes, characterized by convex rounded protrusions or spicules. Another set of agents, including cationic amphipaths, low salt, low pH and cholesterol depletion, induces concave shapes called stomatocytes. These shape responses are universal in the sense that the shapes seen and their order of appearance do not depend on which echinocytogenic or stomatocytogenic agent is used. The RBC consists of a composite membrane including a fluid and asymmetric lipid bilayer in which integral proteins or transmembrane and amphiphilic proteins are diffusing or are immobilized by their non-covalent bindings to peripheral proteins and a flexible membrane skeleton scaffold laminating the cytoplasmic surface of the lipid bilayer and constituted by peripheral proteins. The first explanation for these shape changes was provided by Hoffman [5] and Sheetz and Singer [6] who proposed that the mechanism involves membrane disbalance and small changes in the relaxed area difference ΔA_0 between the two leaflets of the plasma membrane. Thus, any effect that expands the outer leaflet relative to the inner one (increasing ΔA_0) produces a tendency to form convex structures on the cell surface (e.g., echinocytic spicules); conversely, an expansion of the inner leaflet relative to the outer one (decreasing ΔA_0) favors concavities (e.g., stomatocytic shapes). A recently proposed model postulates that the erythrocyte shape is determined by the bending elasticity of the lipid bilayer and shearing and stretching elasticity of the membrane skeleton [7,8]. This so-called bilayer couple concept (BCC) explains the universality of the main, stomatocyte–discocyte–echinocyte or reverse sequences by postulating that all shape changing agents (chemical, or physical) act solely or mainly through their effect on ΔA_0. This model is also able to reproduce the different stages of the echinocytosis and stomatocytosis by a simple variation of the relative areas of the inner and outer leaflets of the lipid bilayer as well as to predict existence of other shapes outside of this main sequence seen under certain conditions [7]. Bilayer couple concept was successfully applied to qualitatively and quantitatively explain RBC shape changes induced by variety of exogenous stimuli [9–14].

An apparent difficulty with these mechanical models is their poor ability of explaining erythrocyte shape changes induced by alterations of pH and ionic composition of the medium [1,15–18]. Erythrocytes equilibrated in altered pH buffers assume altered shapes. Below

Abbreviations: HBS, HEPES-buffered saline; RBC, red blood cells; MR, morphological response; SI, shape index; Cpr, chlorpromazine; SSS, standard sucrose solution; NSVDC, non-selective voltage dependent channel

* Tel.: +38 057 373 0135; fax: +38 057 373 0084.
E-mail address: rsv@kharkov.ua.

0005-2736/$ – see front matter © 2010 Elsevier B.V. All rights reserved.
doi:10.1016/j.bbamem.2010.05.010

external pH 6.0, membrane curvature becomes negative (stomatocytic), above pH 8.0 curvature becomes positive (echinocytic). It has been showed that change in neither cell water nor cell chloride altered the morphology of normal pH cells. In contrast, change in cell pH caused shape change in normal-range membrane potential and cell water content. The results show that change in cytoplasmic pH is both necessary and sufficient for the shape changes and vesiculation [19] of human erythrocytes equilibrated in altered pH environments [16]. Thus, it can be proposed that lowering of intracellular pH decreases ΔA_0 of the membrane bilayer while elevation of pH increases ΔA_0 [15,16]. The problem, however, persists that molecular structures responsible for changes in ΔA_0 remain largely unclear. Several authors have recently proposed that membrane-bound proteins play an active or even dominant role in controlling shape changes [3,17,20].

Wong [3] have suggested that most of amphiphilic compounds, if not all, alter the shape by altering the conformation of Band 3 (AE1 or anion exchanger 1). Indeed, they inhibit the Band 3 anion transport activity, and several of them inhibit the Band 3 anion transport activity and alter the shape concomitantly. The slowly transported Band 3 substrates arsenate, iodide, nitrate, oxalate and vanadate and the specific Band 3 anion transport inhibitors dipyridamole, DIDS and DNDS are echinocytogenic [21–23]. This model differs qualitatively from mechanical models in that the membrane skeleton by its high conformational flexibility is used to generate different shapes and that Band 3 conformation determines the membrane skeleton conformation. This function of the membrane skeleton is consistent with proposals that it plays a more dominant role than the lipid bilayer asymmetry in determining the erythrocyte shape [24,25]. The mechanism predicts shape changes with changes of pH and ionic composition since the Band 3 conformation depends on the Donnan equilibrium ratio of Cl^-, HCO_3^- and H^+ which is influenced by pH and ionic composition. It could explain several other observations directly or indirectly related to the erythrocyte shape, suggesting its plausibility [3,4]. The other view is, however, that bilayer has a dominant role while skeleton plastically accommodates the contours imposed upon it by the overlying membrane [26,27].

Gimsa and Ried [17] have also suggested that the erythrocyte shape transformations produced by pH change are caused by a Band 3 conformational change since they occur too rapidly to be explained by a redistribution of the phospholipids of the lipid bilayer. The results of Betz et al. [20] seem to confirm this suggestion. It should be noted, however, that neither model contradicts to BCC but differing only in recognizing detailed membrane components governing local area expansion or contraction. In the Wong model, conformation of cytoskeleton plays a dominant role whereas in Gimsa model this role belongs to conformational state of imbedded membrane proteins. An important aspect is that these two models are mutually exclusive because according to Wong outward facing conformation of AE1 produces stomatocytes while the opposite is suggested by the other model where this conformation has a larger external cross section producing echinocytes. Hence, only one approach if any should be valid.

Another parameter assumed to affect the RBC shape per se is the transmembrane potential [28,29]. However, the effect of the transmembrane potential is controversial because other authors claimed no causal relationship between membrane potential and cell shape; thus, a possible mechanism still remains unclear [20,21,30–32].

According to BCC, crenated or invaginated forms represent a transitional stage of shape changes that occur classically during discsphere transformations of constant volume [33]. These transformations, going from smooth biconcave discs to spheres can be induced not only by exposure to a variety of surface-active agents but even by a pH gradient [1]. The shape changes are known to take place rapidly (seconds) and can be reversed by removal of the "sphering" agent [1,33]. Spontaneous reversal of the shape change, from spheres back to discs, may occur also in suspensions of cells remaining in the presence of a sphering agent [1,34]. This type of spontaneous reversal was correlated with the equilibrium distribution of the sphering agent between the bulk and cellular phases and were interpreted to indicate that the agent was at equilibrium on the two sides of the membrane [1]. In many special cases, reversion proceeds further to stomatocytic or echinocytic shapes in time and concentration dependent manner. For example, the spiculated McLeod erythrocytes were converted by chlorpromazine into biconcave disks at lower concentration and, at higher concentration, into stomatocytes [35]. Similarly, in spherical erythrocytes from long-preserved blood increase in ATP content is accompanied by a shape change of the cells to discoidal form via a crenated form without volume changes [36]. Sodium salicylate-treated erythrocytes could be returned to normal morphology and normal membrane rheology by addition of chlorpromazine. [37]. In addition, a spontaneous shape change occurs if the cells are in contact with a glass surface [38].

Usually, as predicted by BCC, interaction of RBC with stomatocytic agents resulted in initial echinocytosis with subsequent transformation to discs and further to stomatocytes. However, among the stomatocytic amphiphiles there were some that induced stomatocytosis immediately or after a short lag time while others first passed the erythrocyte through echinocytic stages before stomatocytic shapes were attained [39–41]. Characteristic triphasic time course of shape changes consisting of rapid formation of stomatocytes followed by reversion to discs or echinocytes and then again to stomatocytes was found for RBC having positive transmembrane potential after interaction with CPR [42]. These shape changes lasted about 30 min. Various shape dynamics were observed upon interaction of some anionic and cationic drugs with RBC in media of different chloride content [28,43,44]. Exogenous phospholipids DLPC and DLPS initiated the conversion from echinocytes to stomatocytes which was attributed by selective and energy-dependent translocation of PS to the membrane inner leaflet [40,41]. In all cases, the cell transformation from echinocytes to stomatocytes proceeds via an intermediate discoid shape. The same results were demonstrated for many other short-chain (dilayroil)phospholipid analogues [45].

Finally, many useful examples of echinocyte–stomatocyte transformation induced by variety of conditions can be found in the works of Schwarz et al. [23,46] dealing with RBC modified by electric field pulses. Echinocytes formed from discocytic erythrocytes by electric field pulses at 0 °C return to the discocytic shape upon incubation at 37 °C and subsequently turn into stomatocytes due to an active and passive components of phospholipid translocation. Repetitive pulses at higher field strengths lead to a progressively more discocytic stationary shape during subsequent resealing. This phenomenon was explained by the progressively increased transbilayer mobility of the normally almost immobile phospholipid sphingomyelin and a consecutive progressive symmetrization of all membrane phospholipids [23].

In his review, Nakao [25] listed several points not easily explained by BCC in its simplest form where lipid bilayer alone is responsible for shape changes. These observations, in fact, do not contradict to BCC if composite membrane is taken into account because some alterations during experimental treatments may occur within membrane skeleton as well. In the same way, findings apparently not consistent with BCC found in [39] could be attributed to amphiphile-induced formation of non-bilayer H_{II} phase, conditions that are not described by this model.

Nevertheless, there are some data that on the first glance indeed are difficult to reconcile with BCC. Schwarz et al. [46] showed that extensive membrane modification by repetitive field pulses followed by 20 h incubation at 37 °C produce discocytic cells which are resistant to many established shape-transforming treatments, including single electric field pulses, Ca^{2+} incorporation and exposure to membrane active amphiphiles, metabolic depletion, binding of band 3 ligands, alkaline pH and contact with glass surfaces. Some effects can readily be interpreted by a complete symmetrization of the phospholipids in pulse-modified cells which prevents shape transformations related to the asymmetric

disposition of the phospholipids. The reason of other effects is unclear. Although important, these findings were obtained using modified and leaky, not native, cells. It is possible that such type of modification impairs some part of shape-transforming mechanism and therefore could not be considered as a strong argument against BCC. In summary, it seems there are no at present direct experimental evidences contradicting BCC for native RBC at near physiological environment.

Interestingly, the similar sequence of echinocyte–stomatocyte fast shape changes observed in electroporated cells was found when RBC were placed in isotonic sucrose solution with low amount of phosphate which did not contain any additional constituents able to induce shape changes. Inhibitor of anion transport DIDS substantially inhibited this retransformation [17]. Mechanism of this phenomenon is virtually unknown, although it is well established that RBC assume stomatocytic shape in hypotonic and mixed sucrose–salt solutions [16,17,20,28,29,31] and futures of morphological response have been recently characterized [32].

In this paper, we investigated the dynamics of RBC shape response in simple unbuffered near isotonic sucrose solutions to give new insight on the mechanism of RBC shape changes caused by controlled challenge in cell environment. We identified several shape states of RBC and showed that rather mild changes in cell environment initiated a series of pronounced fast and slow transitions between these states. Some transitions are expected based on BCC whereas other transitions are not expected and seem to be hardly explain by this concept in its direct form pointing to the need for a more complex description of the membrane.

2. Materials and methods

EDTA (tetra and disodium salts) was purchased from Sigma, *N*-(2-Hydroxyethyl)piperazine-*N*′-2-ethanesulfonic acid (HEPES) was from Serva and sucrose from Merck. Ophtalmic reagent Xalacom containing Latanoprost and Timolol was from Pfizer (Belgium). All other reagents were obtained from major suppliers and were of the highest purity available.

2.1. Preparation of erythrocytes

Human blood was withdrawn in vacuum vacutainer tubes with sodium citrate or EDTA as anticoagulants on the day of the experiment from informed volunteers. After free blood sedimentation, 0.15 ml of the red blood cell pellet was transferred into and washed once in 5 ml of physiological saline (PS) (150 mM NaCl) and then once again in 5 ml of HEPES-buffered saline HBS (150 mM NaCl, 5 mM HEPES, pH 7.4). Excess supernatant after the centrifugation was removed to leave 1 ml final volume of red blood cell stock suspension which, if not indicated otherwise, was allowed to stay for 2 h at room temperature before measurements to avoid initial drift in cell properties [32].

2.2. Measurement of dynamics of RBC shape changes

A non-invasive method based on measuring fluctuations of light flow (transmission) through the cell suspension bearing information about cell flatness (or sphericity) was implemented in a two-channel shapemeter–aggregometer SA-01, which was used to monitor time-dependent shape changes of RBC. The principle of the method was published elsewhere [47]. The shape index (SI) was estimated according to the protocol described earlier for shape determination of erythrocytes and calculated by the following expression: $SI = k \times D$, where k is a constant, depending on the amplification of the signal and device calibration, and D is a mean value of light flow fluctuations, averaged in 1-s intervals. The calibration coefficient k can be used to form a scale, allowing to estimate dimensionless SI, which reflect the shape of RBC. It was adjusted so that the value of SI for fresh erythrocytes in HBS was equal 1. Under these conditions, the minimal value of SI which corresponds perfect spheres was ~0.07. The 7–10 μl of RBC from the stock suspension was added to a cylindrical glass cuvette containing 2 ml of HBS to obtain an initial value of absorbance in the range 0.30 ± 0.02. This corresponds to a cell concentration in the cuvette $\sim 6 \times 10^6$ cells in 1 ml. The same amount of cells was added to 2 ml of standard unbuffered 0.3 M sucrose solution (SSS) (pH 5.8–6.2) with mixing at 600 rpm by a small magnetic rod and the recording of the signal started immediately. Due to limitations discussed elsewhere [32], solution of 0.3 M sucrose was used throughout of experiments as standard medium.

2.3. Determination of red blood cells morphology

RBC were fixed by glutaraldehyde directly in the cuvette after desired time of equilibration. The final concentration of glutaraldehyde was usually 0.45% and the fixative contained additionally phosphate buffer which gave 1–2 mM final concentration in the cuvette after dilution, pH 6.0. Steady-state morphology of RBC after 5 min of incubation in the presence of fixative in sucrose media was inspected by light microscopy in thin layer [38]. Data presented in the figures are typical from 3 to 5 independent experiments carried out with blood from different donors. All experiments were performed at room temperature (20–22°C).

3. Results

3.1. Characterization of changes of shape index and absorbance during MR

When RBC are first placed in isotonic sucrose solution with low chloride content dynamic shape response called morphological response (MR) is observed. Generally, it consists of three phases: (i) fast spherulation (phase 1), (ii) restoration of shape close to discoidal one (phase 2), followed by (iii) a second more slow spherulation (phase 3). Fig. 1 shows characteristic examples of changes in absorbance and SI of stirred cell suspension for 3 donors obtained in different experiments. It is seen, that dynamics of changes in both parameters could be varied depending on blood sample and procedure of its preparation, especially on ionic composition of stock solution in which RBC are equilibrated before placing them into sucrose solution. Taking in mind this variability [32] in the present study, we analyzed only samples that show characteristic control shape response like that shown in Fig. 1. Microscopic observation revealed that RBC at the end of phase 2 (when SI reaches its maximal value) appeared as discs, whereas at the end of phase 3 they have a shape of stomatocytes. Direct visualization of actual cell shape in phase 1 is complicated due to rapidity of process at the beginning of MR; however, fixation of samples (see below and data from [32]) revealed a prevalence of echinocytic shapes. Therefore, standard MR represents the following sequence of morphological transformations: discocyte (in HBS) > echinocyte (phases 1 and 2) > discocyte > stomatocyte (phase 3). This morphological transformation is rather a fast process, usually comprises 1- to 2-min interval with peak SI value within 20–30 s. As can be seen from Fig. 1, the morphological response in general is represented by a curve in the shape of wide or narrow peak.

Fig. 1B shows dependence of absorbance versus SI during MR. Two linear parts are clearly visible on these plots. The first line with smaller angle between SI axis and absorbance axis corresponds to phase 2 (increase in SI) while the second line corresponds to phase 3 (larger angle, decrease in SI). Arrows show direction of SI changes during time course of MR. Straight lines indicated represent linear regression fit of experimental data in the form: $\text{absorbance} = b_0 - b_1 \times \text{SI}$ performed in SigmaPlot. Values of b_1, characterizing slope of lines calculated for 3 donors shown in Fig. 1, are as follows: phase 2: $b_1(1) = 0.022$, $b_1(2) = 0.021$, $b_1(3) = 0.022$; phase 3: $b_1(1) = 0.056$, $b_1(2) = 0.047$, $b_1(3) = 0.056$. Therefore, the slope in phase 3 is twice as large as in phase 2 for all donors, although time courses of MR for them are not identical. This mean that MR could proceed with different rate while preserving

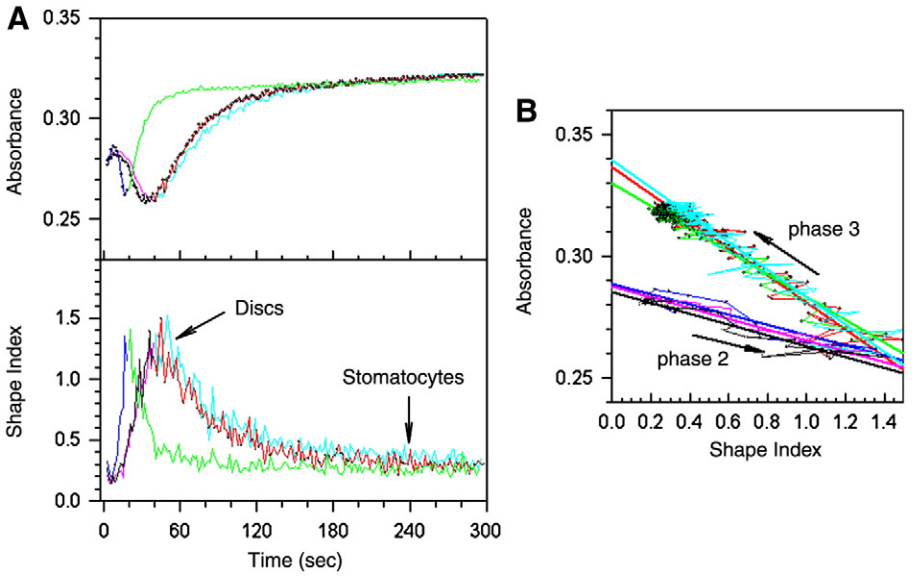

Fig. 1. Characteristic examples of changes in absorbance and SI of erythrocytes versus time (morphological response (MR)) after their transfer into SSS (A) and corresponding dependence of absorbance versus SI (B). Solid lines indicate linear regression fit of data before and after the SI maximum. Arrows indicate direction of SI changes during MR. Each curve corresponds to individual experiment, including separation of red blood cells from different blood samples and preparation of new fresh sucrose solutions.

relationship between absorbance and SI during the whole process. We believe that this conservative relationship can be used to identify the trajectory of shape changes in terms that during discocyte–echinocyte (stomatocyte) transition, each particular shape identified by the value of SI corresponds to certain value of absorbance. The fact that this relation is linear provides a unique possibility to use coefficient b_1 as a parameter characteristic to actual phase of MR. In this paper, we will use this type of analysis based on linear dependence between absorbance and SI (absorbance–SI analysis, ASI) during time course of MR to isolate and identify different morphological states, phases and possible transitions between different states including identification of trajectory, i.e. actual route of cell shape changes during transition from one state to another.

There are at least two reasons why two linear parts on ASI plot have different slopes. The first possibility could be based on assumption that echinocytes and stomatocytes scatter light in a different manner. If so, the same changes in SI during shape changes from discs to echinocytes or stomatocytes will correspond to different changes in absorbance and will lead to different values of slope. For instance, if phase 2 reflects transition from echinocytes to discs, corresponding changes in absorbance are smaller compared to those in phase 3 which corresponds to transition from discs to stomatocytes. This means that at the same degree of sphericity, stomatocytes scatter more light than echinocytes resulting in a larger relative absorbance deflection. The other possibility relates to volume changes of cells in sucrose solution. The absence of external chloride leads to intracellular chloride loss and cell shrinkage [48,49], which is accompanied with increase in absorbance [50]. In phase 3, the cell shrinking is accompanied by disc crenation both leading to increase in absorbance, whereas in phase 2 shrinking is accompanied with reverse shape transformation from sphere to disc, the latter leads to decrease in absorbance. The superposition of these opposite trends can give a smaller resultant absorbance deflection and correspondingly lower value of b_1. It is not excluded that both processes partly contribute to overall changes in absorbance during MR.

Schematic diagram of MR is shown in Fig. 2. Standard MR is considered as a spontaneous sequential morphological transition from discoid shape to final stomatocytic shape. Here S_0 is initial rest discoid shape state of RBC in isotonic physiological solution at normal pH. Placing cells into isotonic sucrose medium with low chloride content initiates shape transition toward the new echinocytic state S_1. This transition proceeds through phase designated as phase 1. After that the cells spontaneously perform additional transitions from S_1 to intermediate discoid state S_2 (phase 2) and further to final stomatocytic state S_3 (phase 3).

The molecular mechanisms and actual reasons why the cells demonstrate such a behavior is not clear. However, from the general point of view based on bilayer couple concept (BCC), the following working hypothesis could be proposed. It is based on the assumption that in sucrose solution the cells experience a combine influence of at least two factors with opposite type of action relative cell shape (echinocytic or stomatocytic) and different rate constants determining temporal characteristics of their action. For example, sucrose solution could be considered as strong but relatively slowly acting stomatocytogenic factor, and there are many confirmations in the literature that shape of RBC in sucrose solutions are usually stomatocytic [16,17,19,20,28,29,31,42]. On the other hand, the absence of chloride in sucrose solution would lead to fast recruitment of AE1 into outward facing external conformation and expansion of external monolayer of membrane resulting in echinocytocis [17,20]. Therefore, after initial echinocytosis (S_1), the permanent stomatocytogenic action of sucrose will cause transition of cells into stomatocytes through discoid shape (S_2) as intermediate in full accordance with BCC. In this case, it is even not important what actual reasons like positive transmembrane potential [28,29] or redistribution

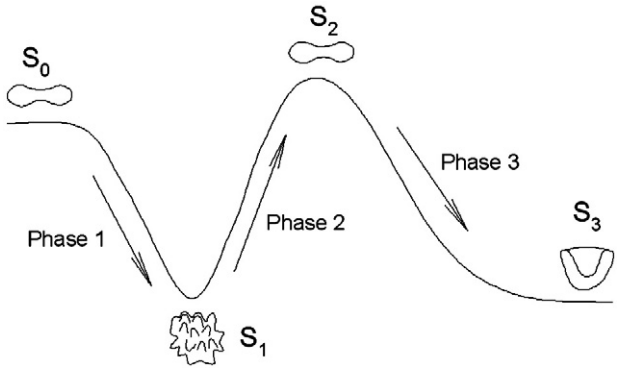

Fig. 2. Schematic diagram of MR. Here S_0 is an initial rest discoid shape state of RBC in isotonic physiological solution at normal pH. S_1—echinocytic state which the cells assume immediately after placing them into isotonic sucrose medium with low chloride content. S_2—intermediate discoid state. S_3—final stomatocytic state. Transition $S_0 \rightarrow S_1$ proceeds through phase designated as phase 1. Similarly, phases 2 and 3 indicate transitions $S_1 \rightarrow S_2$ and $S_2 \rightarrow S_3$, respectively.

of some membrane components [40] underline stomatogenic action of sucrose. Based on this preliminary schematic representation of MR, one may suppose theoretically an existence of other possible transitions between different shape states of RBC which are presented in Table 1 (see discussion). In general, 12 possible transitions between 4 main shape states may exist. Three of them constitute of standard MR. According to Fig. 2 and BCC, other transitions between adjacent states could be easily imaged if some additional factor acts in corresponding direction relative to actual shape state. For example, transition $S_3 \rightarrow S_2$ is expected if echinocytic agent is added which compensates stomatocytosis in state S_3. Similarly, the same agent added at state S_2 should initiate transition $S_2 \rightarrow S_1$ or inhibit transformation toward S_3. However, the existence of more complex transitions such as $S_3 \rightarrow S_1$ or $S_3 \rightarrow S_0$, etc., should be established experimentally. If exists, these transitions could represent a difficulty for BCC to explain their origin and mechanism based solely on area differences in both membrane monolayers.

3.2. Instability of state S_2: transition $S_2 \rightarrow S_1 \rightarrow S_2 \rightarrow S_3$

Since second discoid shape in state S_2 during MR is temporal, we first investigated the possibility of other transitions from this state except normally occurring transition toward state S_3. The example of transitions induced by changes in pH is shown in Fig. 3. Aliquots of NaOH needed to increase pH on approximately 0.5 (curve 2) or 1 (curve 1) pH unit were added at the SI peak position, i.e. in state S_2. In both cases, increasing pH initiated rapid transformation of cells into spheres in direct proportion to magnitude of pH increase.

This latter transformation in turn was unstable and was completed by series of additional transitions resembling standard MR. Because basic pH is considered as echinocytic factor, the shift from discoid state S_2 to echinocytic state S_1 could be suggested. This is confirmed by ASI analysis showing that corresponding parameters b_1 for phase 2 ($b_1 = 0.0229$) and phase 3 ($b_1 = 0.0422$) of the second peak closely correspond to those of control MR. This implies that shift in pH in basic direction "reset" shape state S_1 and initiates new series of shape changes. Because total change in absorbance during this process including second pH-induced peak is larger compared to control MR without pH shifts, one may conclude that pH-induced shape transformation proceeds with additional volume changes.

3.3. Effect of NaCl, calcium, citrate and pH shift on different phases of MR

Data presented in Fig. 4 show effects of increasing ionic strength and application of citrate at final shape state of MR S_3 as well as an action of calcium at the very beginning of process and an acid pH shift applied in state S_2. Corresponding ASI plots are shown in Fig. 5.

Adding NaCl to the cells in state S_3 (150 s after beginning of MR) resulted in slow increase of SI indicating returning cell shape to disc. This reversibility did not depend on time which the cells spent in sucrose solution because similar restoration of SI was detected when NaCl was added in 75 or 450 s after the cells. ASI analysis (Fig. 5A) shows that SI reversal follows almost the same trajectory as direct transition from S_2 to S_3 during MR despite the fact that absolute values of absorbance depended on time of cell equilibration in sucrose. The latter is attributed to more pronounced shrinkage of cells at longer equilibration period. Probably due to volume changes the final value of absorbance after shape restoration does not coincide with corresponding initial value in state S_2 both having similar SI. Taking in mind that parameter b_1 has the same value during direct and reverse transitions, one can suggest that NaCl induces restoration of state S_2 in which the cells have slightly reduced volume. On the other hand, it is not excluded that actually this new discoid state represents S_0. Indeed, if the value b_1 for direct transition $S_3 \rightarrow S_2$ is close to that of $S_3 \rightarrow S_0$, then ASI analysis is unable to distinguish between them.

To investigate a possible role of volume changes, we compared a magnitude of absorbance and SI in sucrose solutions containing 20 mM NaCl. As seen in Fig. 6, both the absorbance and SI have the same values in state S_2 during MR and in discoid state when NaCl was added to sucrose prior the cells. In the latter case, triphasic MR is absent (see Fig. 7B, SI2, tracks 3 and 4) and the cells have large SI indicating discoid shape. Absorbance is higher and SI is lower when NaCl was added 150 s after the cells showing incomplete restoration of cell shape and volume. In other experiments with different blood samples, the complete restoration of SI could be attained, which nevertheless corresponds to higher value of absorbance.

These data show that in media with equal composition, the same values of SI correspond to different values of absorbance, most probably attributed to volume decrease. It should be noted that adding NaCl at SI peak position inhibited phase 3 (see below) and did not change absorbance, further suggesting that at these circumstances NaCl inhibited volume changes also. These data could be interpreted in a manner that NaCl could either abolish sucrose-induced volume changes or even reverse them. Therefore, NaCl restores discoid shape of cells in parallel with partial restoration of volume which cells had at the moment of NaCl addition. This imply that injection the cells into NaCl–sucrose solution does not substantially change the shape and volume of cells at least within first 2–5 min of incubation, and therefore the cells are probably in the same state S_0 as in electrolyte physiological saline. However, the question what state S_0 or S_2 the cells are entering after NaCl addition in sucrose solution requires further elucidation (see below).

Data presented in Fig. 4 show that in the presence of Ca^{2+} (or at low pH, not shown), there is no visible phase 1 and the rate of shape changes is reduced. Therefore, in these media, the cells demonstrate only transition toward final state S_3 with b_1 value corresponding to phase 3 ($b_1 = 0.049$ for both cases). Similar result was obtained in the presence of Na2EDTA (50 μM) with value $b_1 = 0.047$, which also tends to lower pH of solution (not shown). Based on these finding, we can assume that under these circumstances the cells do not enter into state S_1 but rather undergo direct transition from S_0 to S_2 and further to S_3. This could be expected because low pH [15,16,18] and probably Ca^{2+} [51] are stomatocytic and compete with echinocytosis in phase 1. On the other hand, it could be expected that the rate of phase 3 would be increased owing to combine action of sucrose and low pH or Ca^{2+}. This is not confirmed in the experiment because the rate of phase 3 is even lower compared to control suggesting more complex mechanism than pure additive effect. Inhibition of phase 1 by Ca^{2+} or low pH did not prevent NaCl-induced flattening of RBC (Fig. 4); however, the rate and extent of restoration was smaller compared to that in the absence of Ca^{2+} and at pH 6.0 (not shown).

Table 1
Possible transitions between RBC shape states.

Main state	Transition	Characteristic and conditions	b_1	End state probing test	
				DIDS	ΔpH
S_0				Responsive	Unresponsive
	$S_0 \rightarrow S_1$	Phase 1	0.05		
	$S_0 \rightarrow S_2$	+ NaCl, + Ca^{2+}		Fixing	Responsive
	$S_0 \rightarrow S_3$	Shown in [42]			
S_1					
	$S_1 \rightarrow S_0$	?			
	$S_1 \rightarrow S_{0A}$	Oxalate		Responsive	Responsive
	$S_1 \rightarrow S_2$	Phase 2	0.022		
	$S_1 \rightarrow S_3$	Shown in [56]			
S_2				Fixing	Responsive
	$S_2 \rightarrow S_0$	Rare		Responsive	Unresponsive
	$S_2 \rightarrow S_1$	Basic pH shift, oxalate, citrate			
	$S_2 \rightarrow S_3$	Phase 3	0.051		
S_3					
	$S_3 \rightarrow S_0$	Oxalate, Xalacom		Responsive	
	$S_3 \rightarrow S_1$	Basic ΔpH			
	$S_3 \rightarrow S_2$	NaCl		Fixing	Responsive

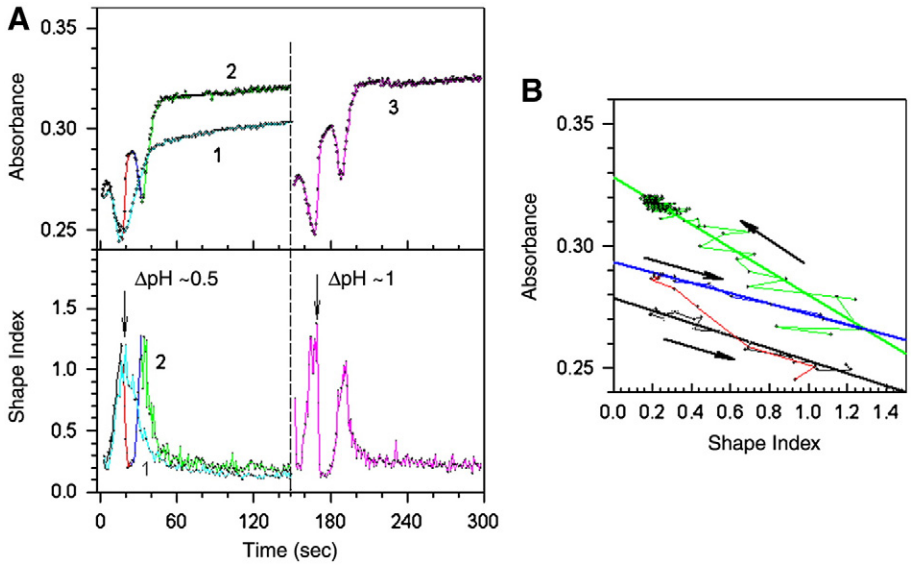

Fig. 3. Effect of basic pH shift applied in state S_2 of MR on subsequent dynamics of shape changes (curves 2 and 3). The arrows in A show moment of NaOH addition in order to increase pH of the media approximately by 0.5 or 1 pH unit. Curve 1 corresponds to standard MR without pH changes. (B) Absorbance–SI plot corresponding to curve 2 in A. The arrows indicate direction of SI changes during MR and after increase in pH. Similar plot was obtained for curve 3 (not shown).

More complex shape transitions were found when cells environment was changed in state S_3. Moderate increase in pH initiated complex shape response including transient phases (probably fast swelling as judged from abrupt decrease in absorbance). Remarkably, the subsequent time courses of absorbance and SI changes were nearly identical to initial MR except of increased absorbance (Fig. 7A, SI2). Fig. 5C clearly shows equal slopes of absorbance–SI dependencies for corresponding phases during shape transformation. Practically the same results was obtained for Na4EDTA (50 μM) which also slightly increased pH of sucrose. Lowering pH at this 150-s point reduced SI further and did not cause large additional time-dependent changes in absorbance and SI (not shown). Due to identical behavior of both absorbance and SI during the second pH or Na4EDTA-induced shape wave, we suggest that in order to do that the cells should undergo direct transition from stomatocytic state S_3 again to state S_1 without reaching an intermediate discoid shape. The other possibility is that transformation into the discs proceeds very quickly (in fraction of second) and could not be registered. This is true for measurements of SI those are limited by integration intervals in 1 s. However, the time resolution of absorbance is much higher (20 ms). Since shape changes are reflected in both absorbance and SI, the absence of fast changes in absorbance sufficient to accommodate discoid shape makes the presence of this intermediate shape less probable. According to our scheme (Fig. 2), transition $S_3 \rightarrow S_1$ indicates that stomatocytes with high degree of sphericity (low SI) are rapidly and continuously transformed into echinocytes with near the same sphericity and therefore change the sign of membrane curvature from negative (concave) to positive (convex).

Data from Fig. 4 show that at low concentration, citrate initiates transition which could be recognized as $S_3 \rightarrow S_2 \rightarrow S_3$. In contrast to

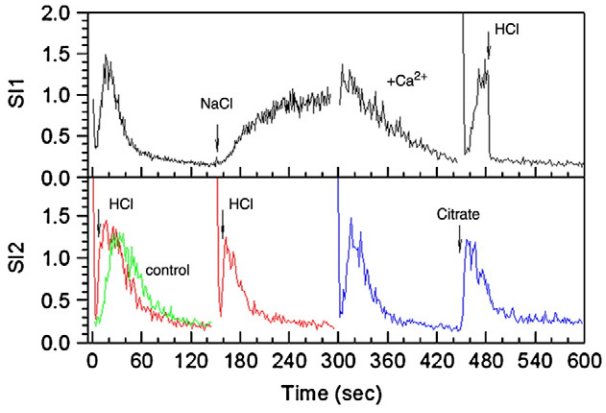

Fig. 4. Effect of NaCl, $CaCl_2$, NaOH, HCl and citrate on time course of SI changes during MR. Arrows show moment of addition of reagents at final concentration in mM: NaCl 20, $CaCl_2$ 0.5, citrate 0.1. Amounts of NaOH and HCl were adjusted in order to increase or decrease pH of the media approximately by 1 pH unit, respectively. Labels with (+) indicate that reagents were added to the media prior the cells. Control curve in SI2 is shown for comparison.

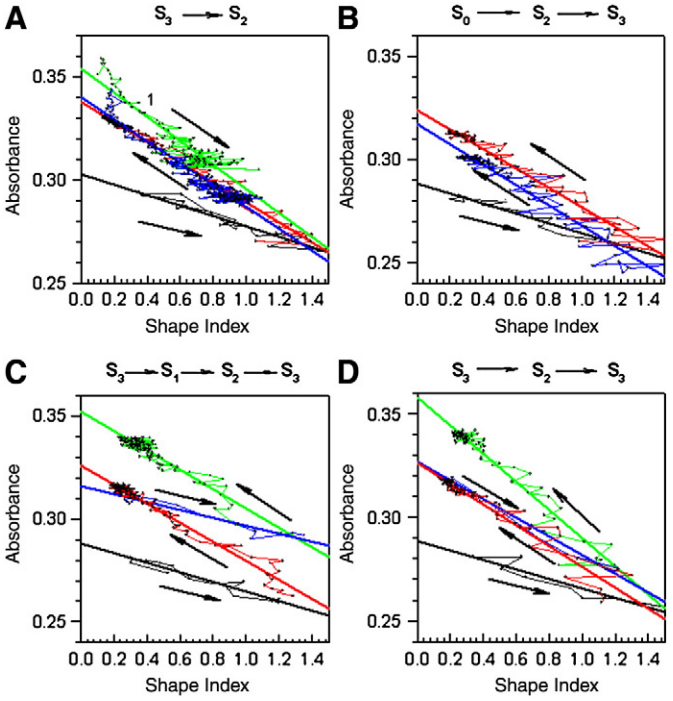

Fig. 5. ASI plots corresponding to data presented in Figs. 4 and 7A (SI2). The arrows indicate direction of SI changes during MR and after addition of reagents. (A) NaCl; (B) $CaCl_2$; (C) NaOH; (D) citrate. Curve 1 in A corresponds to the shape restoration of cells which were equilibrated in sucrose solution for 450 s before addition of NaCl.

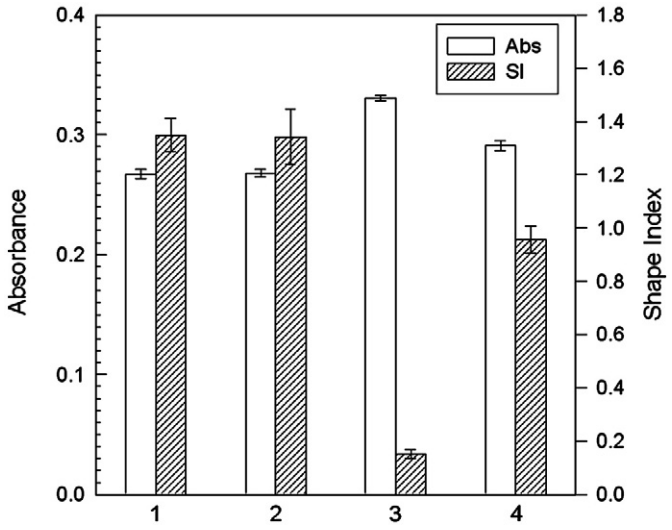

Fig. 6. Absorbance (open bars) and SI (filled bars) of cell suspension in state S_2 (1), state S_3 (3), when NaCl was added to sucrose solution prior the cells (2) and after NaCl-induced reversion of state S_3 (4). The data are shown as mean ± SD, $n = 4$. Concentration of NaCl is 20 mM.

transition $S_3 \rightarrow S_2$ induced by NaCl (Fig. 4) which proceeds slowly, citrate initiated very rapid (within several seconds) restoration of discoid shape. This restoration follows almost the same trajectory (Fig. 5D) as initial direct transition $S_2 \rightarrow S_3$ with slightly lower value of b_1 (0.044 vs. 0.048). The similar results confirming reversible reversal of S_3 in the order $S_3 \rightarrow S_2 \rightarrow S_3$ were obtained also with oxalate, salicylate and tartrate when appropriate concentrations of reagents were used (not shown).

3.4. Effect of pH on dynamics of MR

If BCC can be used to describe general futures of MR, taking in mind schematic representation of process (Fig. 2), we can make a prediction that stomatocytic agent acting at the end of phase 1 (state S_1) should facilitate the transition $S_1 \rightarrow S_2 \rightarrow S_3$. When considering stomatocytic agent in nonelectrolyte solution, it should be taken into account the chemical nature of agent. In fact, being stomatocytic in physiological salt solution such an agents could demonstrate diverse effects under hyperpolarization conditions [42–44]. For instance, chlorpromazine as a classical stomatocytic agent cannot be used to verify the above proposal under present experimental conditions [52]. We therefore additionally explored an effect of low pH which as well known induces stomatocytosis [15,16,18] and inhibited phase 1. In accordance with prediction data from Fig. 4, it shows that lowering pH in 5 s after beginning of MR, i.e. at state S_1, accelerates both phases 2 and 3 proportionally to acidification of the external medium.

The same pH lowering at peak value (state S_2) (Fig. 4, SI1, track 3) greatly stimulated phase 3 especially when the shift in pH was increased, whereas changing pH at state S_3 produced almost no effect (not shown). These findings confirm the suggestion that low pH and sucrose act in the same stomatocytic direction and low pH potentiates the effect of sucrose. Surprisingly, this potentiation occurs, however, only when pH drop is applied after beginning of MR not before them. In addition, total change of absorbance (difference between maximal and minimal values during MR at standard interval in 150 s) at low pH was smaller ($\Delta A = 0.03$) compared to that of normal pH ($\Delta A = 0.05$). The latter could indicate that shape transformation at low pH proceeds with limited volume changes that is consistent with the observations that low pH induces swelling of the cells [16]. Qualitatively similar results were obtained with calcium at concentrations 0.1–0.5 mM (not shown). The fact that lowering pH or adding Ca^{2+} in 5 s after beginning of MR

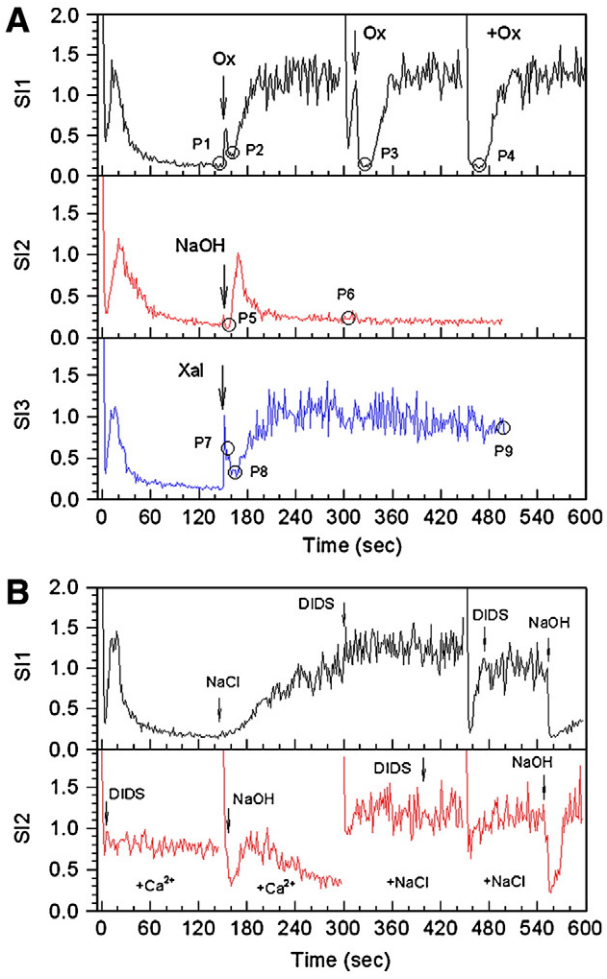

Fig. 7. Characteristic examples of morphological response and effects of oxalate, NaOH and Xalacom on time course of RBC shape changes in SSS (A) and effects of NaCl, $CaCl_2$, NaOH and DIDS added in some temporal points during MR (B). (A) The arrows show moment of addition of oxalate at final concentration 2 mM, NaOH to increase pH in 1 U or 6 μl Xalacom (for content see Materials and Methods) to 2 ml of RBC suspension. Critical points P1–P9 correspond to time points in which fixative containing glutaraldehyde was added in order to fix actual shape of RBC in these points for subsequent microscopic examination. (B) Final concentrations of NaCl 10 mM, $CaCl_2$ 0.5 mM, and DIDS 20 μM. Labels with (+) indicate that reagents were added to the media prior the cells.

accelerates phases 2 and 3 whereas eliminates phase 1 and inhibits phase 3 when injecting the cells into calcium-containing or low pH media suggests that all these phases could be regulated independently.

3.5. Microscopic verification of RBC shape in critical points of MR

Fig. 7A illustrates several examples of MR where ASI analysis can make some important predictions about actual shape of RBC in certain time points during MR shown in the Figure. Adding oxalate to the cells in state S_3 results in abrupt decrease in absorbance and increase in SI followed by subsequent time-dependent changes in these parameters. Although qualitatively similar to changes induced by pH, this response is different because SI jumps immediately (without delay) after oxalate addition. After that, it reaches the minimum before restoration to final maximal value corresponding to discs. ASI analysis has shown that last phase of MR after oxalate addition has the value b_1 close to that of control phase 2. Because phase 2 usually follows phase 1 it could be expected that the phase between the moment of oxalate addition and SI minimum represents phase 1. If so, the state in which the cells are entered immediately after oxalate addition should be S_0.

In standard MR, the phase 1 is rather fast to detect mainly due to limitation (~1.5 s) to reach homogeneous distribution of cells in the cuvette after injection. Therefore, we do not know the value of parameter b_1 for this phase. In the presence of oxalate, the presumable phase 1 became longer (~10 s) allowing to estimate b_1. We found that the value b_1 of phase 1 is close to that of phase 3 (~0.05). Therefore, ASI analysis predicts that stomatocytic shape in point P1 should be transformed by oxalate into echinocytic shape in point P2 designating transition $S_3 \rightarrow S_0 \rightarrow S_1$. Similarly oxalate induces transition $S_2 \rightarrow S_1 \rightarrow S_2$ being added at SI peak position (point P3) and stabilizes state S_1, producing a lag when initially present in the medium (point P4). It is expected that at all these points the cells assume echinocytic shape. These expectations have been confirmed by the microscopic analysis of samples fixed in corresponding time points directly in the cuvette during MR (Fig. 8). In contrast to point P1 where only stomatocytes can be found at terminal phase of MR, points from 2 to 4 contain many echinocytes in excellent agreement with ASI analysis. This analysis also predicts direct conversion of stomatocytes into echinocytes without intermediate discoid shape which occurs after pH increase in phase 3 leading to a second wave of nearly identical MR (Fig. 7A, SI2). We therefore expected to find echinocytes immediately after basic shift of pH (point P5) that was also confirmed by microscopy (Fig. 8, P5). Importantly, these echinocytes were spontaneously transformed into the discs and further to stomatocytes as visualized in point P6.

According to ASI analysis and corresponding time course of MR, the action of Xalacom was similar to that of oxalate. Indeed, exclusively echinocytes were found in the minimum of SI (point P8) after Xalacom addition and discocytes after restoration of SI (point P9) in the presence of Xalacom, respectively. The mixed populations of RBC containing echinocytes, stomatocytes and discs (point P7) or echinocytes and stomatocytes (point P5) or echinocytes and discs were revealed immediately after Xalacom addition, pH shift and addition of oxalate (point P2).

3.6. Possible existence of other transitions: $S_0 \rightarrow S_3$; $S_1 \rightarrow S_0$; $S_2 \rightarrow S_0$; $S_1 \rightarrow S_3$ and probing test to distinguish between S_0 and S_2

The foregoing results directly demonstrate an existence of eight transitions between some shape states according to scheme shown in Fig. 2. The main difficulty in assessing possibility of other transitions arise from the fact that two states S_0 and S_2 are discoid and transitions between them are undetectable by the present technique. It is a question; is it correct to consider S_0 and S_2 as different states? Taking this in mind, we performed an additional attempts to distinguish between these discoid states. We saw above that prerequisite of state S_2 is a high sensitivity to basic pH shift (Fig. 3). In addition, data from Fig. 7B (SI1, track 2) show that 20 μM DIDS is able to fix this state completely inhibiting phase 3. So, in general, this state is ΔpH responsive and DIDS fixing. Even after fixing by DIDS, this state is still ΔpH responsive. In contrast, in physiological saline (150 mM NaCl) state S_0 is DIDS responsive and ΔpH unresponsive (not shown). Therefore, these two states are principally different in their response to DIDS and ΔpH. As shown in Fig. 7B, the states S_2 predicted by ASI analysis and arising after shape restoration induced by NaCl or in the presence of 0.5 mM Ca^{2+} both have the same future. The first result confirms the transition $S_3 \rightarrow S_2$ whereas the second points to transition $S_0 \rightarrow S_2$ which occurs in the presence of Ca^{2+} at the beginning of MR. When NaCl is added to the medium before the cells, the resulting state is again S_2 because it is ΔpH responsive and DIDS fixing (Fig. 7B, SI2, tracks 3 and 4), indicating the same transition $S_0 \rightarrow S_2$.

Our DIDS probing test additionally confirmed an existence of short lived state S_0, not S_2 after oxalate addition in state S_3 (150 s after the

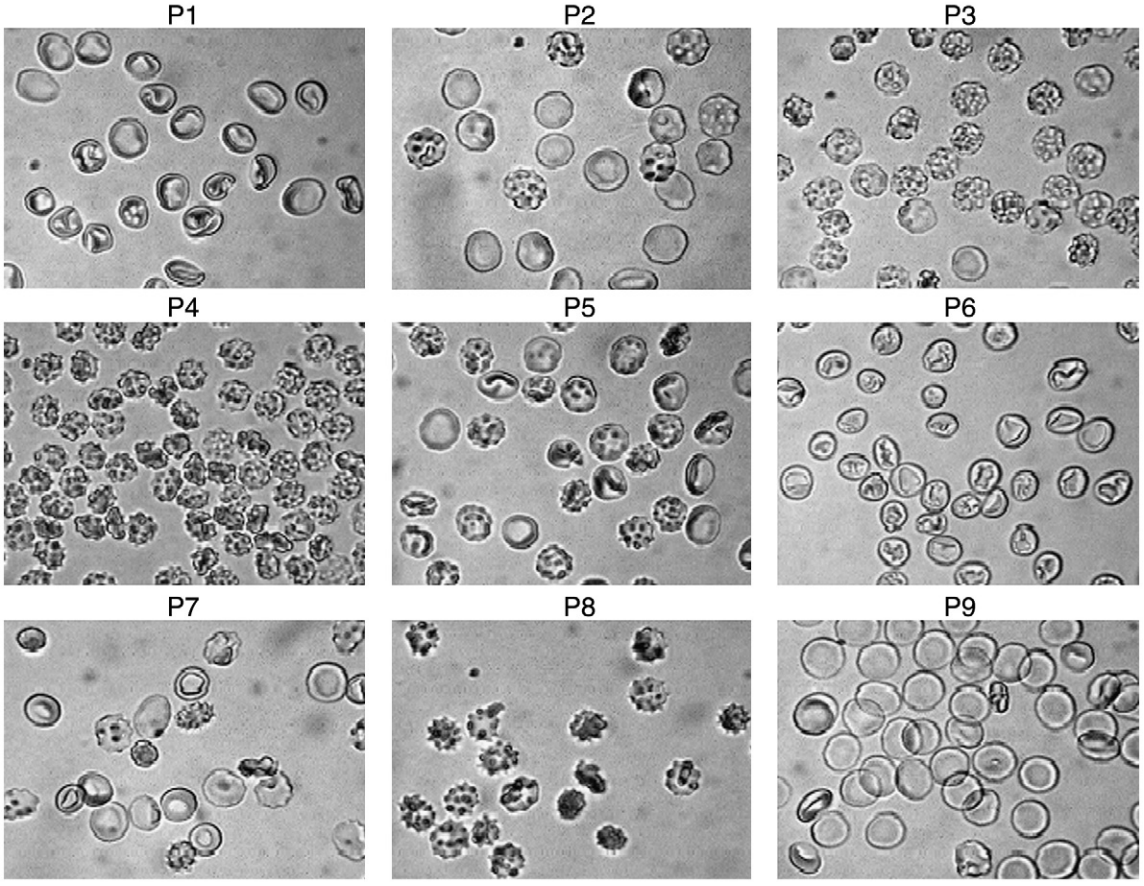

Fig. 8. Morphology of fixed RBC in critical points P1–P9 shown in Fig. 7A. Initial magnification, ×800.

cells, Fig. 7A (SI1, track 1)). When DIDS was added at this second sharp peak, i.e. in 2 s after the oxalate, it immediately decreased SI and inhibited subsequent shape restoration. Again, addition of DIDS just prior the oxalate did not influence this peak but again inhibited SI changes after the peak (not shown). These results strongly suggest that this intermediate peak reflects DIDS-responsive state S_0, not S_2, which, in contrast, is DIDS fixing, thus confirming ASI predictions. An interesting finding was that final discoid shape that cells assume in the presence of oxalate (Fig. 7A, SI1, track 2 and 3) possesses both DIDS and ΔpH sensitivity and therefore this state is not a pure S_0 or S_2 state. It seems possible to consider this special state as substate of S_0 (S_{0A}) which become also ΔpH responsive. In some our experiments, we found that state S_2 can be converted into S_0 when NaCl is added in MR peak position, because the final state become DIDS responsive and ΔpH unresponsive that corresponds to S_0 in physiological saline. However, reproducibility of these results was pure and underlying reason for that it is not clear. Nevertheless, this is an indication that states S_0 and S_2 could be mutually converted in each other under some circumstances. Thus, probing the actual state by DIDS and ΔpH can help in distinguishing between S_0 and S_2 states in sucrose solution.

4. Discussion

In discussing the present data, some general remarks should be done. (1) BCC having clear physical background could be applied to human RBC, a flexible cell devoid from developed intracellular cytoskeleton network having composite membrane within the limits of rather small surface perturbations provided the functional state of membrane remains in large extent intact. In this case, RBC can be considered as a giant filled vesicle which shape is under control of relative surface difference between leaflets of composite viscoelastic membrane [53], (2) decisive conclusions as for compatibility of BCC to description of real shape dynamics could not be made from experiments in which membrane structure was impaired or changed by experimental maneuvers like the treatment the cells by detergents, ionophores, enzymes, electrical breakdown and so forth without detailed knowledge of mechanism of action of perturbants. For example, we believe that conclusion about relationship between RBC shape and transmembrane potential could not be conclusively inferred only from experiments with ionophores due to uncertainties in the effect of ionophore itself.

The purpose of the given work was to characterize dynamic shape transitions (morphological response, MR) of native erythrocytes upon their introduction into a nonelectrolyte medium containing or not rather small amount of other constituents like chloride, citrate, oxalate, calcium, etc. The shape index used by us to assess the morphology of RBC cannot distinguish the actual shape of cells when they are not discoid in contrast to the morphological index [16,17,40,41]; however, SI could be recorded continuously with high precision and time resolution that gives an additional benefit in constructing ASI plots. The use of SI is better suited to analyze data in terms of deviation of the cell shape from discs, bearing in mind that these changes could be in echinocytic or stomatocytic directions.

Schematic diagram of the process is shown in Fig. 2 where the phase 1 is echinocytic (state S_1) and phase 3 is stomatocytic (state S_3). In terms of explaining the foregoing results, we proposed a working model based on BCC that cell shape changes are the result of influence of at least two factors acting simultaneously. One factor (factor 1) is echinocytic and acts rapidly whereas other factor (factor 2) is stomatocytic and acts slowly compared to the first one but overall it has stronger shape transforming potential.

Even more simple model including only one factor could be suggested that MR is a result of inward transmembrane translocation of some membrane component (e.g. PS) initially exposed to extracellular leaflet of membrane as a result of contact with sucrose [41], the idea similar to behavior of cell after electrical breakdown [23,46,54]. Both models can satisfactory explain the main sequence of shape changes during MR as well as the following observations:

(1) Increasing pH (echinocytic) in discoid state S_2 produced echinocytes, whereas decreasing pH (stomatocytic) rapidly produced final stomatocytosis. When pH was lowered at echinocytic state S_1, this results in fast retransformation toward discs and then to stomatocytes with increased rate.
(2) Injection of cells into the media containing stomatocytic Ca^{2+} [51] or low pH value [15] inhibited initial echinocytosis as predicted.
(3) Addition of echinocytic salicylate or tartrate or small increase in pH at stomatocytic state S_3 induced rapid transient conversion to discs followed by returning to stomatocytes.

The observations confirming rather fast initial crenation followed by retransformation to discs and stomatocytes retarded by DIDS have been briefly reported in [17]. These data are consistent with proposed scheme and do not contradict BCC because echinocytes produced by DIDS strengthens echinocytic action of factor 1 at the beginning of MR.

The transition echinocyte–disc–stomatocyte is a classical transition predicted by BCC and confirmed in many experiments with substances having a preference to incorporate into inner monolayer of membrane [6,10,12,39–41,47,55]. Removing of external agent could produce transition in reverse order [1]. Transition could be reversed adding an agent with opposite type of action [47,55]. In both cases, crenation and invagination occurred through an intermediate disc shape. Under more complex conditions stomatocytes could be directly transformed into echinocytes [55], but reverse transition is impossible without hemolysis. Actually, these facts are not accepted by BCC; however, one should take into account non-physiological conditions under which such effects take place, as discussed above. Our previous experiments have shown that transitions between stomatocytes induced by chlorpromazine and echinocytes induced by lysolecithin could proceed in both directions via discs as intermediate form precisely depending on concentrations of reagents used and without hemolysis [47].

However, the following results obtained in this study are not consistent with the models:

(1) NaCl induced shape restoration at any stage of phase 3 (transition $S_3 \rightarrow S_2$) and therefore behave like an echinocytic agent. However, in contrast to this expectation NaCl strongly inhibited rather than activated echinocytic phase 1. This effect can be explained as a result of influence of ionic strength or lowering of positive transmembrane potential on phase 3 of MR as well as possible influence of chloride on inhibition of phase 1.
(2) Initial low pH like NaCl and calcium inhibited phase 1 that is consistent with its stomatocytic action. However, at those conditions, low pH and calcium did not accelerate stomatocytic phase 3 as expected and really occurred when pH was lowered in 5 s after cells injection in standard medium (Fig. 4, SI2, tracks 1 and 2). Probably these cases reflect significance of ionic environment at initial stage of MR.
(3) Our results show existence of rare direct transition between stomatocytes and echinocytes without intermediate discoid shape under mild environment conditions induced by moderate increase in pH. pH per se is not considered as a strong perturbing factor in the physiological range; however, at pHs higher that 8.0 and lower than 5.5, the cells will crenate and invaginate, respectively [15,16]. Therefore, based on BCC, increasing pH in state S_3 is expected to be echinocytic and should reduce the degree of stomatocytosis leading to shape changes in discs direction in a manner similar to that of NaCl. Instead, the cells instantaneously adopted echinocytic shape followed by spontaneous conversion to discs and further on to stomatocytes resembling pH response in state S_2 (compare

Figs. 4 and 7). The latter implies that proposed stomatocytic factor 2 has a permanent action in time which is consistent with view that it could be a positive transmembrane potential. In general, it seems that cell response on basic shift in pH principally does not depend on actual phase and state of the cells during MR. Even injection the cells into media with elevated pH resulted in the same type of reaction. This is in a great contrast with mode of action of other substances where the result does really depend on RBC state (e.g. oxalate, Fig. 7A, SI1).

(4) While both low concentrations of citrate and oxalate initiated fast return of stomatocytic cells from state S_3 to discs (S_2) as predicted by BCC only for oxalate (echinocytic agent) and contradict to citrate (stomatocytic agent), a larger concentrations of both appear to stimulate a more complex transition directly to S_0 followed by starting MR from the very beginning ("reset" phenomenon). It is important to note in this respect that threshold concentrations of organic anions and some inorganic anions producing initial visible effect on different stages of MR are small enough and comparable to those of surface-active agents and detergents while otherwise they are not considered as strong shape perturbing factors at least at such low concentrations. For instance, initial effective concentrations for acetate, oxalate, salicylate and tartrate were in the range 150–250 μM and those for ions CO_3^-, HCO_3^-, H^+, OH^-, citrate and Na4EDTA in the range 10–25 μM. All these findings are not easily to be explained by BCC implying more complex mechanisms involved.

Hoffman [1] showed that in HIS the sphere is an intermediate form in conversion of RBC shape from one state to another during pH shifts in both acid and base directions. Our data are consisted with this view only for basic shift in mixed sucrose–NaCl solutions (Fig. 7B, SI2, track 4) and additionally provide the evidence that in pure LIS this response is asymmetric with discs as an intermediate forms and futures of only acid shifts are compatible with the statements of BCC. Some authors defined that shape transformation and cell volume are almost unrelated to each other [1,15,21,25,36]. This is also true for MR because discoid shape can be attained at different volumes as visualized in ASI plots.

Our main findings are summarized in Table 1 where some properties of four basic states and 12 possible transitions between them are indicated. We have shown for the first time that two states S_0 and S_2 both being discoid nevertheless are different in their response to probing by DIDS and pH shift. Further we have shown experimentally that almost all set of possible transitions between neighbour or remote states in a sequence shown in Fig. 2 could exit under appropriate external conditions. Recently we have shown an existence of transition $S_1 \rightarrow S_3$ induced by acid pH shift in the presence of benzalkonium chloride. In contrast to transition $S_3 \rightarrow S_1$ where spherostomatocyte could be transformed directly into spheroechinocyte the reverse transition was accompanied by some flattening of the cell which nevertheless did not assume discoid shape [56]. Transition $S_0 \rightarrow S_3$ induced by chlorpromazine in mixed sucrose–NaCl solution has been reported elsewhere [42]. The only transition which has not been identified yet is a transition $S_1 \rightarrow S_0$. Probably this transition requires rather special external environment.

Because red blood cells are not damaged in simple sucrose solution, containing only very few amount of other constituents, we believe that the data presented here are the first direct evidence against BBC. This concept does not allow direct transitions between remote non-discoid shapes as well as it does not suppose an existence of two and even more discoid states S_0, S_{0A} and S_2. Therefore, we have to find more realistic description of mechanisms governing red blood cells shape.

The fact that RBC assume stomatocytic shape in sucrose solutions is well known for many years but reasons for this still remain obscure. Some explanations were proposed including membrane depolarization [28,29] and counter ion binding [31]. From our data it is clear that a strong membrane depolarization is not a first causal factor leading to MR. If it was so, one would expect only limited shifts in the initial sphering of the cells (phase 1) under conditions in which a large inside positive potential is formed. Moreover, positive transmembrane potential is considered as stomatocytic agent [28,29], whereas the initial shape of RBC during in MR is echinocytic. Ca^{2+} at low concentrations (0.1–0.5 mM) and low pH strongly inhibited phase 1, although at low pH potential is even higher than that at neutral pH [57,58]. Obviously, the initial transmembrane potentials in these cases were not substantially different; however, MR was. Therefore, at the same high positive potential the cells could be echinocytes, discocytes and stomatocytes. Involvement of increased surface potential of membrane in LIS [57] and adsorption of counterions [31] can explain only final stomatocytic shapes of RBC in hypotonic and LIS media but not an existence of multiple transitions especially when changes in ionic strength are very low (Fig. 7). One of the possible explanation of MR is based on the fact that LIS induced fast alkalization of RBC cytoplasm due to rapid Cl^- loss which was followed by a slower cell acidification due to operation of $K^+(Na^+)/H^+$ exchanger in the human erythrocyte membrane [49]. This Cl^- loss and increase in intracellular pH was inhibited by anion transport inhibitors. Our pH data generally are consistent with suggested apparent correlation between intracellular pH and cell shape. Increase and decrease in pH_i during MR correlate with echinocytosis and stomatocytosis, respectively (Figs. 3 and 4). However, DIDS inhibiting elevation in pH_i [49] did not inhibit echinocytes formation while retarded retransformation forward stomatocytes [17] suggesting a more complex relationship. In addition, unbuffered sucrose solution produces only limited, if any, changes in pH_i due to buffer capacity of intracellular hemoglobin. Therefore, it seems that MR proceeds at virtually the same intracellular pH and poorly depends on initial pH_i value [32]. Additional work is needed to clarify more precisely relationship between intracellular pH and cell shape in LIS.

Since MR is revealed under conditions when normally silent transport pathways are activated, it is reasonable to suppose that NSVDC and/or $K^+(Na^+)/H^+$ exchanger could take a part, but the exact role of these systems is difficult to evaluate at present because some their features do not show a correlation with MR. For example, it was shown that NSVDC channel activation was blocked by a decrease of the intracellular but not the extracellular pH with the apparent pK(A) value for the effect was estimated to be 6.5 [48], whereas MR is strongly dependent on extracellular pH shifts. $K^+(Na^+)/H^+$ exchanger is strongly activated in sucrose solutions containing Tris buffer and less activated in tartrate [49], whereas MR is inhibited in the presence of Tris [32]. Tartrate demonstrated complex response resembling that of citrate and oxalate (not shown). It is known that in normal erythrocytes, osmotic shock, oxidative stress, energy depletion and Cl^- removal activate Ca^{2+}-permeable cation channels with Ca^{2+}-induced suicidal erythrocyte death, i.e. surface exposure of phosphatidylserine, cell shrinkage and membrane blebbing which was significantly increased in cells lacking AE1 [59]. Unusual dependence of MR on Ca^{2+} application makes the involvement of this channel and subsequent biochemical events resulting in KCl loss, activation of phospholipase A_2 and sphingomyelinase, formation of ceramide and phospholipid scrambling of the cell membrane [60,61] probable also. Although contradictory, the involvement of aforementioned transport pathways in MR could be a basis for explanation why some principal observations are not consistent with BCC. This is in line with the ability of ceramide to form microdomains, which coalesce into larger platforms or macrodomains (rafts), facilitate signal transduction initiated by the specific stimulus [62] and are central for the spatial organization of receptors and signaling molecules [63]. MR therefore could be based on redistribution of rafts in the plane of RBC membrane.

A peculiar feature of MR and especially additional morphological responses on subsequent changes in cell environment is that they are

fast processes occurring within 1–2 s or less in the nominal absence of additional substances that themselves could affect the shape of RBC. It is hardly to imagine that these fast morphological transformations of RBC are attributable to transmembrane redistribution of membrane lipids because this is usually rather slow compared to the rate of shape changes observed [17,58]. Echinocyte formation in electrically porated cells is most likely caused by the reorientation of endofacial aminophospholipids to the outer leaflet of the bilayer and proceeds longer [54]. If initial echinocytosis in MR is attributed by similar mechanism, it is not clear how small shifts in pH or concentrations of inorganic and organic anions could dramatically and in some cases instantaneously affect this reorientation (Figs. 3, 4, 7). Besides, electroporated cells has been shown to be unresponsive to some shape transforming stimuli [23,46]. In contrast, RBC in sucrose solution are even extra responsive to stimuli which otherwise produced no effect in salt salines (citrate, oxalate, small pH deflections, not shown). Nevertheless, it cannot be completely excluded at present that some part in the mechanism of MR belongs to fast transmembrane redistribution since it is known that cholesterol [64], free fatty acids [65,66] and ceramides [67] cross the membrane rather quickly.

Gimsa and Raid [17] suggested that the initial echinocytocis in LIS is a result of recruitment of AE1 sites to an outward facing conformation. This conformation is believed to have larger external cross section and produce an expansion of outer monolayer of membrane [20]. Although reasonable, this proposal meets difficulties in explaining specific blocking effect of calcium and low pH (Fig. 4) implying that recruitment alone is not a sufficient background. This aspect of MR also directly contradicts to the model of shape regulation proposed by Wong [3,4] because his model suggests that outward conformation of AE1, E_0 leads to expansion of cytoskeleton network producing stomatocytic shapes. Thus, the true reasons leading to initial echinocytosis in phase 1 of MR still remain obscure.

Of course our scheme of MR depicted in Fig. 2 is the simplest one to describe this phenomenon. It is not excluded that shape of RBC can assume more than four basic states. The basis for this suggestion is the identification of substate of S_0 (S_{0A}) and observations that in some experiments with different blood samples we identified discoid states which were both DIDS and ΔpH responsive or instead DIDS and ΔpH unresponsive. This could be interpreted in a manner that discoid states S_0 and S_2 have different substates, e.g. S_{0A}, S_{2A}, etc., differing in sensitivity to DIDS and pH shift. Identification of these additional states and their role in RBC morphological transformations awaits future elucidation.

It is known that human erythrocytes are equipped with a diversity of receptors and effectors that mediate well-characterized signal transduction pathways in nonerythroid cells [68].

Morphological and volume alterations of human erythrocytes caused by the anion transporter inhibitors has been assigned to AE1-mediated transmembrane signaling which leads to altered cytoskeleton dynamics [69]. Binding of ligands to the extracellular region of the erythrocyte transmembrane protein glycophorin A induced a decrease in membrane deformability. Since the property of membrane deformability is regulated by the skeletal proteins on the cytoplasmic side of the membrane, this suggests that ligand binding may initiate a transmembrane signal. Both the extracellular domain to which the ligand binds and the cytoplasmic domain of glycophorin A have been shown to be a crucial for this process [70]. Any transmembrane signaling mechanism suggests an existence of specific sensor which first come in contact with corresponding stimuli. In the study of pH equilibration in human red blood cell suspension, it has been suggested that the species dominating pH equilibration is probably dependent on the extracellular pH, which determines the magnitude of the driving gradient for each H^+ and OH^- ions, the idea close to the existence of extracellular pH sensor on RBC membrane [71]. This corresponds to experimental results that kinetics of the Cl–pH equilibration in human red blood cells depends strongly on the kind and the concentration of the buffer system used [72]. In the other work, it was concluded that protons inhibit erythrocyte K–Cl cotransport through internal histidine(s) which may be part of a pH sensor [73]. A pH sensor was also identified for rabbit and human chloride channels [74]. In order to regulate their volume, the cells should sense volume changes, generate signals upon cell volume alterations and transfer these signals to the transport systems executing sell volume regulation [75]. Monovalent ions may serve as second messengers in these responses although the molecular origin of sensors involved remains unknown [76]. Since MR is accompanied with both volume changes and redistribution of chloride, potassium and protons, it is reasonable to suggest that these fluxes in combination with pH and volume sensor mechanisms could be involved in the actual mechanism of this phenomenon.

Finally, it is not excluded that some shape effects could be attributed to direct interactions between RBC membrane and sucrose itself. Janoshazi et al. [77] showed that the human red cell glucose transport protein and AE1 are in close enough contact that information can be transmitted from the glucose transport protein to AE1 as well as in opposite direction. Disaccharide caused a time-dependent biphasic enhancement of tryptophan fluorescence in fresh red cells, which was modulated by the specific anion exchange inhibitor, DBDS (4,4'-dibenzamido-2,2'-stilbene disulfonate), and depended upon specific disaccharide conformation, indicating that these effects could be attributed to a site sensitive to sugar conformation. Probably this is a basis to explain why MR is so critical to composition of sucrose solution as well as a source of sucrose [32].

Therefore, it could be suggested that MR represents a phenomenon in which the major role can play pH and chloride-sensitive sensor and switching mechanisms coupled with transmembrane signaling thus involving both cytoskeleton and membrane in coordinated shape response on changes in cell ionic environment.

References

[1] J.F. Hoffman, On the mechanism and measurement of shape transformations of constant volume of human red blood cells, Blood Cells 12 (1987) 565–588.
[2] J.F. Hoffman, Some red blood cell phenomena for the curious, Blood Cells Mol. Dis. 32 (2004) 335–340.
[3] P. Wong, A basis of echinocytosis and stomatocytosis in the disc-sphere transformations of the erythrocyte, J. Theor. Biol. 196 (1999) 343–361.
[4] P. Wong, A hypothesis of the disc-sphere transformation of the erythrocytes between glass surfaces and of related observations, J. Theor. Biol. 233 (2005) 127–135.
[5] J.F. Hoffman, Quantitative study of factors which control shape transformations of human red blood cells of constant volume, Nouv. Rev. Fr. Hématol. 12 (1972) 771–774.
[6] M.P. Sheetz, S.J. Singer, Biological membranes as bilayer couples. A molecular mechanism of drug–erythrocyte interactions, Proc. Natl. Acad. Sci. USA 71 (1974) 4457–4461.
[7] H.W.G. Lim, M. Wortis, R. Mukhopadhyay, Stomatocyte–discocyte–echinocyte sequence of the human red blood cell: evidence for the bilayer-couple hypothesis from membrane mechanics, Proc. Natl. Acad. Sci. USA 99 (2002) 16766–16769.
[8] R. Mukhopadhyay, H.W.G. Lim, M. Wortis, Echinocyte shapes: bending, stretching, and shear determine spicule shape and spacing, Biophys. J. 82 (2002) 1756–1772.
[9] L.M. Chi, W.G. Wu, Effective bilayer expansion and erythrocyte shape change induced by monopalmitoyl phosphatidylcholine. Quantitative light microscopy and nuclear magnetic resonance spectroscopy measurements, Biophys. J. 57 (1990) 1225–1232.
[10] J.E.J. Ferrell, K.J. Lee, W.H. Huestis, Membrane bilayer balance and erythrocyte shape: a quantitative assessment, Biochemistry 24 (1985) 2849–2857.
[11] M.P. Sheetz, R.G. Painter, S.J. Singer, Biological membranes as bilayer couples. III. Compensatory shape changes induced in membranes, J. Cell Biol. 70 (1976) 193–203.
[12] M.P. Sheetz, S.J. Singer, Equilibrium and kinetic effects of drugs on the shapes of human erythrocytes, J. Cell Biol. 70 (1976) 247–251.
[13] A. Iglic, V. Kralj-Iglic, H. Hagerstrand, Amphiphile induced echinocyte–spheroechinocyte transformation of red blood cell shape, Eur. Biophys. J. 27 (1998) 335–339.
[14] Y. Lange, J.M. Slayton, Interaction of cholesterol and lysophosphatidylcholine in determining red cell shape, J. Lipid Res. 23 (1982) 1121–1127.
[15] M.M. Gedde, E. Yang, W.H. Huestis, Shape response of human erythrocytes to altered cell pH, Blood 86 (1995) 1595–1599.
[16] M.M. Gedde, D.K. Davis, W.H. Huestis, Cytoplasmic pH and human erythrocyte shape, Biophys. J. 72 (1997) 1234–1246.
[17] J. Gimsa, C. Ried, Do band 3 protein conformational changes mediate shape changes of human erythrocytes? Mol. Membr. Biol. 12 (1995) 247–254.

[18] M. Rasia, A. Bollini, Red blood cell shape as a function of medium's ionic strength and pH, Biochim. Biophys. Acta 1372 (1998) 198–204.
[19] M. Gros, S. Vrhovec, M. Brumen, S. Svetina, B. Zeks, Low pH induced shape changes and vesiculation of human erythrocytes, Gen. Physiol. Biophys. 15 (1996) 145–163.
[20] T. Betz, U. Bakowsky, M.R. Muller, C.M. Lehr, I. Bernhardt, Conformational change of membrane proteins leads to shape changes of red blood cells, Bioelectrochemistry 70 (2007) 122–126.
[21] E.M. Bifano, T.S. Novak, J.C. Freedman, Relationship between the shape and the membrane potential of human red blood cells, J. Membr. Biol. 82 (1984) 1–13.
[22] D.M. Hoefner, M.E. Blank, D.F. Diedrich, The anion transporter and a 28 kDa protein are selectively photolabeled by *p*-azidobenzylphlorizin under conditions that alter RBC morphology, flexibility, and volume, Biochim. Biophys. Acta 1327 (1997) 231–241.
[23] S. Schwarz, B. Deuticke, C.W. Haest, Passive transmembrane redistributions of phospholipids as a determinant of erythrocyte shape change. Studies on electroporated cells, Mol. Membr. Biol. 16 (1999) 247–255.
[24] A. Elgsaeter, B.T. Stokke, A. Mikkelsen, D. Branton, The molecular basis of erythrocyte shape, Science 234 (1986) 1217–1223.
[25] M. Nakao, New insights into regulation of erythrocyte shape, Curr. Opin. Hematol. 9 (2002) 127–132.
[26] J.K. Khodadad, R.E. Waugh, J.L. Podolski, R. Josephs, T.L. Steck, Remodeling the shape of the skeleton in the intact red cell, Biophys. J. 70 (1996) 1036–1044.
[27] Y. Lange, A. Gough, T.L. Steck, Role of the bilayer in the shape of the isolated erythrocyte membrane, J. Membr. Biol. 69 (1982) 113–123.
[28] R. Glaser, T. Fujii, P. Muller, E. Tamura, A. Herrmann, Erythrocyte shape dynamics: influence of electrolyte conditions and membrane potential, Biomed. Biochim. Acta 46 (1987) S327–S333.
[29] R. Glaser, Does the transmembrane potential (Deltapsi) or the intracellular pH (pHi) control the shape of human erythrocytes? Biophys. J. 75 (1998) 569–570.
[30] M.M. Gedde, W.H. Huestis, Membrane potential and human erythrocyte shape, Biophys. J. 72 (1997) 1220–1233.
[31] K.D. Tachev, K.D. Danov, P.A. Kralchevsky, On the mechanism of stomatocyte-echinocyte transformations of red blood cells: experiment and theoretical model, Colloids Surf. B Biointerfaces 34 (2004) 123–140.
[32] S.V. Rudenko, Characterization of morphological response of red blood cells in sucrose solution, Blood Cells Mol. Dis. 42 (2009) 252–261.
[33] E. Ponder, Hemolysis and Related Phenomena, Grune and Stratton, New York, 1948.
[34] E. Alhanaty, M.P. Sheetz, Control of the erythrocyte membrane shape: recovery from the effect of crenating agents, J. Cell Biol. 91 (1981) 884–888.
[35] J.K. Khodadad, R.S. Weinstein, L.W. Marsh, T.L. Steck, Shape determinants of McLeod acanthocytes, J. Membr. Biol. 107 (1989) 213–218.
[36] M. Nakao, K. Hoshino, T. Nakao, Constancy of cell volume during shape change of erythrocytes induced by increasing ATP content, J. Bioenerg. Biomembr. 13 (1981) 307–316.
[37] A. Chabanel, W. Reinhart, S. Chien, Increased resistance to membrane deformation of shape-transformed human red blood cells, Blood 69 (1987) 739–743.
[38] L.E. Eriksson, On the shape of human red blood cells interacting with flat artificial surfaces—the 'glass effect', Biochim. Biophys. Acta 1036 (1990) 193–201.
[39] B. Isomaa, H. Hagerstrand, G. Paatero, Shape transformations induced by amphiphiles in erythrocytes, Biochim. Biophys. Acta 899 (1987) 93–103.
[40] D.L. Daleke, W.H. Huestis, Incorporation and translocation of aminophospholipids in human erythrocytes, Biochemistry 24 (1985) 5406–5416.
[41] D.L. Daleke, W.H. Huestis, Erythrocyte morphology reflects the transbilayer distribution of incorporated phospholipids, J. Cell Biol. 108 (1989) 1375–1385.
[42] J. Hartmann, R. Glaser, The influence of chlorpromazine on the potential-induced shape change of human erythrocyte, Biosci. Rep. 11 (1991) 213–221.
[43] A. Nwafor, W.T. Coakley, Drug-induced shape change in erythrocytes correlates with membrane potential change and is independent of glycocalyx charge, Biochem. Pharmacol. 34 (1985) 3329–3336.
[44] A. Nwafor, W.T. Coakley, Charge-independent effects of drugs on erythrocyte morphology, Biochem. Pharmacol. 35 (1986) 953–957.
[45] Smriti, E.C. Nemergut, D.L. Daleke, ATP-dependent transport of phosphatidylserine analogues in human erythrocytes, Biochemistry 46 (2007) 2249–2259.
[46] S. Schwarz, C.W. Haest, B. Deuticke, Extensive electroporation abolishes experimentally induced shape transformations of erythrocytes: a consequence of phospholipid symmetrization? Biochim. Biophys. Acta 1421 (1999) 361–379.
[47] S.V. Rudenko, J.H. Crowe, F. Tablin, Determination of time-dependent shape changes in red blood cells, Biochemistry (Mosc.) 63 (1998) 1385–1394.
[48] P. Bennekou, T.L. Barksmann, P. Christophersen, B.I. Kristensen, The human red cell voltage-dependent cation channel. Part III: distribution homogeneity and pH dependence, Blood Cells Mol. Dis. 36 (2006) 10–14.
[49] D. Kummerow, J. Hamann, J.A. Browning, R. Wilkins, J.C. Ellory, I. Bernhardt, Variations of intracellular pH in human erythrocytes via K(+)(Na(+))/H(+) exchange under low ionic strength conditions, J. Membr. Biol. 176 (2000) 207–216.
[50] J.D. Bisognano, J.A. Dix, P.R. Pratap, T.S. Novak, J.C. Freedman, Proton (or hydroxide) fluxes and the biphasic osmotic response of human red blood cells, J. Gen. Physiol. 102 (1993) 99–123.
[51] M.P. Sheetz, Cation effects on cell shape, Prog. Clin. Biol. Res. 17 (1977) 559–567.
[52] S.V. Rudenko, Low concentration of extracellular hemoglobin affects shape of 1134 RBC in low ion strength sucrose solution, Bioelectrochemistry 75 (2009) 19–25.
[53] R. Grebe, M.J. Zuckermann, Erythrocyte shape simulation by numerical optimization, Biorheology 27 (1990) 735–746.
[54] M.M. Henszen, M. Weske, S. Schwarz, C.W. Haest, B. Deuticke, Electric field pulses induce reversible shape transformation of human erythrocytes, Mol. Membr. Biol. 14 (1997) 195–204.
[55] W.H. Reinhart, S. Chien, Echinocyte–stomatocyte transformation and shape control of human red blood cells: morphological aspects, Am. J. Hematol. 24 (1987) 1–14.
[56] S.V. Rudenko, M.K Saeid, Reconstruction of erythrocyte shape during modified morphological response, Biochemistry (Moscow) (in press).
[57] I. Bernhardt, E. Donath, R. Glaser, Influence of surface charge and transmembrane potential on rubidium-86 efflux of human red blood cells, J. Membr. Biol. 78 (1984) 249–255.
[58] J. Libera, T. Pomorski, P. Muller, A. Herrmann, Influence of pH on phospholipid redistribution in human erythrocyte membrane, Blood 90 (1997) 1684–1693.
[59] A. Akel, C.A. Wagner, J. Kovacikova, R.S. Kasinathan, V. Kiedaisch, S. Koka, S.L. Alper, I. Bernhardt, T. Wieder, S.M. Huber, F. Lang, Enhanced suicidal death of erythrocytes from gene-targeted mice lacking the Cl-/HCO(3)(−) exchanger AE1, Am. J. Physiol. Cell Physiol. 292 (2007) C1759–C1767.
[60] F. Lang, K.S. Lang, P.A. Lang, S.M. Huber, T. Wieder, Osmotic shock-induced suicidal death of erythrocytes, Acta Physiol.(Oxf.) 187 (2006) 191–198.
[61] P.A. Lang, D.S. Kempe, S. Myssina, V. Tanneur, C. Birka, S. Laufer, F. Lang, T. Wieder, S.M. Huber, PGE(2) in the regulation of programmed erythrocyte death, Cell Death Differ. 12 (2005) 415–428.
[62] C.R. Bollinger, V. Teichgraber, E. Gulbins, Ceramide-enriched membrane domains, Biochim. Biophys. Acta 1746 (2005) 284–294.
[63] A.E. Cremesti, F.M. Goni, R. Kolesnick, Role of sphingomyelinase and ceramide in modulating rafts: do biophysical properties determine biologic outcome? FEBS Lett. 531 (2002) 47–53.
[64] T.L. Steck, J. Ye, Y. Lange, Probing red cell membrane cholesterol movement with cyclodextrin, Biophys. J. 83 (2002) 2118–2125.
[65] F. Kamp, D. Zakim, F. Zhang, N. Noy, J.A. Hamilton, Fatty acid flip-flop in phospholipid bilayers is extremely fast, Biochemistry 34 (1995) 11928–11937.
[66] K. Broring, C.W. Haest, B. Deuticke, Translocation of oleic acid across the erythrocyte membrane. Evidence for a fast process, Biochim. Biophys. Acta 986 (1989) 321–331.
[67] I. Lopez-Montero, N. Rodriguez, S. Cribier, A. Pohl, M. Velez, P.F. Devaux, Rapid transbilayer movement of ceramides in phospholipid vesicles and in human erythrocytes, J. Biol. Chem. 280 (2005) 25811–25819.
[68] G. Minetti, P.S. Low, Erythrocyte signal transduction pathways and their possible functions, Curr. Opin. Hematol. 4 (1997) 116–121.
[69] M.E. Blank, D.M. Hoefner, D.F. Diedrich, Morphology and volume alterations of human erythrocytes caused by the anion transporter inhibitors, DIDS and *p*-azidobenzylphlorizin, Biochim. Biophys. Acta 1192 (1994) 223–233.
[70] J.A. Chasis, M.E. Reid, R.H. Jensen, N. Mohandas, Signal transduction by glycophorin A: role of extracellular and cytoplasmic domains in a modulatable process, J. Cell Biol. 107 (1988) 1351–1357.
[71] A.M. Critz, E.D. Crandall, pH equilibration in human erythrocyte suspensions, J. Membr. Biol. 54 (1980) 81–88.
[72] B. Muller, R. Glaser, The kinetics of the Cl–pH equilibration in human red blood cells, Biomed. Biochim. Acta 43 (1984) 77–83.
[73] P.K. Lauf, N.C. Adragna, Functional evidence for a pH sensor of erythrocyte K–Cl cotransport through inhibition by internal protons and diethylpyrocarbonate, Cell. Physiol. Biochem. 8 (1998) 46–60.
[74] K. Stroffekova, E.Y. Kupert, D.H. Malinowska, J. Cuppoletti, Identification of the pH sensor and activation by chemical modification of the ClC-2G Cl-channel, Am. J. Physiol. 275 (1998) C1113–C1123.
[75] A.A. Mongin, S.N. Orlov, Mechanisms of cell volume regulation and possible nature of the cell volume sensor, Pathophysiology 8 (2001) 77–88.
[76] S.N. Orlov, P. Hamet, Intracellular monovalent ions as second messengers, J. Membr. Biol. 210 (2006) 161–172.
[77] A. Janoshazi, G. Kifor, A.K. Solomon, Conformational changes in human red cell membrane proteins induced by sugar binding, J. Membr. Biol. 123 (1991) 191–207.